International Conference on Nuclear Data for Science and Technology 2007
DOI: 10.1051/ndata:07690

Invited

Neutron resonance spectroscopy at n_TOF at CERN

F. Gunsing[1,a], U. Abbondanno[2], G. Aerts[1], H. Álvarez[3], F. Álvarez-Velarde[4], S. Andriamonje[1], J. Andrzejewski[5], P. Assimakopoulos[†6], L. Audouin[7], G. Badurek[8], P. Baumann[9], F. Bečvář[10], E. Berthoumieux[1], F. Calviño[11], M. Calviani[12,13], D. Cano-Ott[4], R. Capote[14,15], C. Carrapiço[1,16], P. Cennini[17], V. Chepel[18], E. Chiaveri[17], N. Colonna[19], G. Cortes[20], A. Couture[21], J. Cox[21], M. Dahlfors[17], S. David[7], I. Dillmann[22], C. Domingo-Pardo[22,23], W. Dridi[1], I. Duran[3], C. Eleftheriadis[24], M. Embid-Segura[4], L. Ferrant[†7], A. Ferrari[17], R. Ferreira-Marques[18], K. Fujii[2], W. Furman[25], I. Goncalves[18], E. González-Romero[4], F. Gramegna[12], C. Guerrero[4], B. Haas[26], R. Haight[27], M. Heil[22], A. Herrera-Martinez[17], M. Igashira[28], E. Jericha[8], F. Käppeler[22], Y. Kadi[17], D. Karadimos[6], D. Karamanis[6], M. Kerveno[9], P. Koehler[29], E. Kossionides[30], M. Krtička[10], C. Lampoudis[1,24], H. Leeb[8], A. Lindote[18], I. Lopes[18], M. Lozano[15], S. Lukic[9], J. Marganiec[5], S. Marrone[19], T. Martínez[4], C. Massimi[31], P. Mastinu[12], A. Mengoni[14,17], P.M. Milazzo[2], C. Moreau[2], M. Mosconi[22], F. Neves[18], H. Oberhummer[8], S. O'Brien[21], J. Pancin[1], C. Papachristodoulou[6], C. Papadopoulos[32], C. Paradela[3], N. Patronis[6], A. Pavlik[33], P. Pavlopoulos[34], L. Perrot[1], M.T. Pigni[8], R. Plag[22], A. Plompen[35], A. Plukis[1], A. Poch[20], J. Praena[12], C. Pretel[20], J. Quesada[15], T. Rauscher[36], R. Reifarth[27], C. Rubbia[37], G. Rudolf[9], P. Rullhusen[35], J. Salgado[16], C. Santos[16], L. Sarchiapone[17], I. Savvidis[24], C. Stephan[7], G. Tagliente[19], J.L. Tain[23], L. Tassan-Got[7], L. Tavora[16], R. Terlizzi[19], G. Vannini[31], P. Vaz[16], A. Ventura[38], D. Villamarin[4], M.C. Vincente[4], V. Vlachoudis[17], R. Vlastou[32], F. Voss[22], S. Walter[22], M. Wiescher[21], and K. Wisshak[22]

The n_TOF Collaboration (www.cern.ch/ntof)

[1]CEA/Saclay-DSM/DAPNIA, Gif-sur-Yvette, France – [2]Istituto Nazionale di Fisica Nucleare, Trieste, Italy – [3]Universidade de Santiago de Compostela, Spain – [4]Centro de Investigaciones Energeticas Medioambientales y Tecnologicas, Madrid, Spain – [5]University of Lodz, Lodz, Poland – [6]University of Ioannina, Greece – [7]Centre National de la Recherche Scientifique/IN2P3-IPN, Orsay, France – [8]Atominstitut der Österreichischen Universitäten, Technische Universität Wien, Austria – [9]Centre National de la Recherche Scientifique/IN2P3-IReS, Strasbourg, France – [10]Charles University, Prague, Czech Republic – [11]Universidad Politecnica de Madrid, Spain – [12]Istituto Nazionale di Fisica Nucleare, Laboratori Nazionali di Legnaro, Italy – [13]Dipartimento di Fisica, Università di Padova, Italy – [14]International Atomic Energy Agency (IAEA), Nuclear Data Section, Vienna, Austria – [15]Universidad de Sevilla, Spain – [16]Instituto Tecnológico e Nuclear (ITN), Lisbon, Portugal – [17]CERN, Geneva, Switzerland – [18]LIP-Coimbra & Departamento de Fisica da Universidade de Coimbra, Portugal – [19]Istituto Nazionale di Fisica Nucleare, Bari, Italy – [20]Universitat Politecnica de Catalunya, Barcelona, Spain – [21]University of Notre Dame, Notre Dame, USA – [22]Forschungszentrum Karlsruhe GmbH (FZK), Institut für Kernphysik, Germany – [23]Instituto de Física Corpuscular, CSIC-Universidad de Valencia, Spain – [24]Aristotle University of Thessaloniki, Greece – [25]Joint Institute for Nuclear Research, Frank Laboratory of Neutron Physics, Dubna, Russia – [26]Centre National de la Recherche Scientifique/IN2P3-CENBG, Bordeaux, France – [27]Los Alamos National Laboratory, New Mexico, USA – [28]Tokyo Institute of Technology, Tokyo, Japan – [29]Oak Ridge National Laboratory, Physics Division, Oak Ridge, USA – [30]NCSR, Athens, Greece – [31]Dipartimento di Fisica, Università di Bologna, and Sezione INFN di Bologna, Italy – [32]National Technical University of Athens, Greece – [33]Institut für Isotopenforschung und Kernphysik, Universität Wien, Austria – [34]Pôle Universitaire Léonard de Vinci, Paris-La Défense, France – [35]CEC-JRC-IRMM, Geel, Belgium – [36]Department of Physics-University of Basel, Switzerland – [37]Università degli Studi Pavia, Pavia, Italy – [38]ENEA, Bologna, Italy

Abstract. Neutron resonance spectroscopy plays an important role in the investigation of neutron induced reaction cross sections and nuclear structure in the MeV excitation range. Neutron time-of-flight facilities are the most used installations to explore neutron resonances. In this paper we describe the basic features of neutron resonance spectroscopy together with recent results from the time-of-flight facility n_TOF at CERN.

1 Introduction

The study of neutron-induced reactions is of large importance in a wide variety of research fields, ranging from stellar nucleosynthesis [1,2], symmetry breaking effects in compound nuclei [3,4], and the investigation of nuclear level densities [5–7], to applications of nuclear technology [8–11], including the transmutation of nuclear waste, accelerator driven systems and nuclear fuel cycle investigations.

The cross sections of neutron-induced reactions can show variations of several orders of magnitude on an energy scale of only a few eV. The origin of these resonances is related to the excitation of nuclear states in the compound nuclear system formed by the neutron and the target nucleus, at excitation energies lying above the neutron binding energy of typically several MeV. The typical time scale $\tau = 10^{-16}$ s of these compound reactions is much slower than in direct reactions as the opposite reaction mechanism.

At these high excitation energies for nuclei of medium and heavy mass the nuclear system is extremely complex and no nuclear model is capable of predicting the position and other

[a] Presenting author, e-mail: gunsing@cea.fr

©2008 CEA, published by EDP Sciences

Article available at http://nd2007.edpsciences.org or http://dx.doi.org/10.1051/ndata:07690

properties of these excited states. Cross sections can therefore only be accessed by measurements.

Due to extreme configuration mixing, the nucleus in this regime above the neutron threshold has a statistical behaviour. This is expressed by the assumption that the matrix elements relating nuclear states have a random character, governed by a Gaussian distribution with zero mean. This statistical model of the compound nucleus is referred to as the Gaussian Orthogonal Ensemble (GOE) [12–15].

The statistical model has direct consequences on the observables of the reaction cross sections. The channel widths are proportional to the square of the matrix elements and have therefore a chi-squared distribution with one degree of freedom, also called the Porter-Thomas distribution. Indeed it has been shown that the distribution of reduced neutron widths follow such a distribution for many nuclei. The observed gamma width of a resonance is in reality the sum of many, for medium and heavy nuclei several tens of thousand, individual gamma widths and tends therefore to follow more a Gaussian distribution. Observed fission widths correspond to a relatively small number of fission channels, at maximum three or four. The resulting distribution can be approximated by an effective chi-squared distribution with a small, fractional number of degrees of freedom.

Today's commonly used formalism which links the physical properties of the nuclear levels to resonance reaction cross sections is the *R*-matrix formalism [16–19], most often in one of its approximations suited for neutron induced cross sections, like the Reich-Moore approximation.

The resonance region, which is the energy region where individual states are excited, can be conveniently divided in a resolved resonance region (RRR) and an unresolved resonance region (URR), where the thermal region around 25 meV is part of the RRR. The boundary between resolved and unresolved resonances is rather fuzzy. One could define this point as the energy where the width of the resonances starts to be larger than the level spacing, but in practice, resonances are unresolved at a much lower energy because of broadening effects, principally Doppler broadening and experimental resolution broadening. The *R*-matrix description can be extended to the unresolved resonance region, where average resonance parameters can be adjusted to describe the cross sections. A different approach in this energy region and at higher energies is the use of optical model calculations.

As an example we show in figure 1 the total neutron-induced reaction cross section for several nuclei of increasing mass. Since the level density increases with mass, resonances are more closely spaced for heavier nuclei and the URR starts at lower energies. But near a closed shell nucleus like ^{208}Pb, the level density is much lower, and we observe the first resonance at a much higher energy.

Indeed resonance data are an important calibration point for all level density models. The extraction of the level density just above the neutron binding energy requires a careful interpretation of the resonance data, including spin and parity assignments and missing level corrections [20,21]. A compilation of experimentally observed resonance data can be found in refs. [22,23] for example.

In evaluated nuclear data libraries, such as BROND, CENDL, ENDF, JEFF, JENDL, and others [24], RRR data

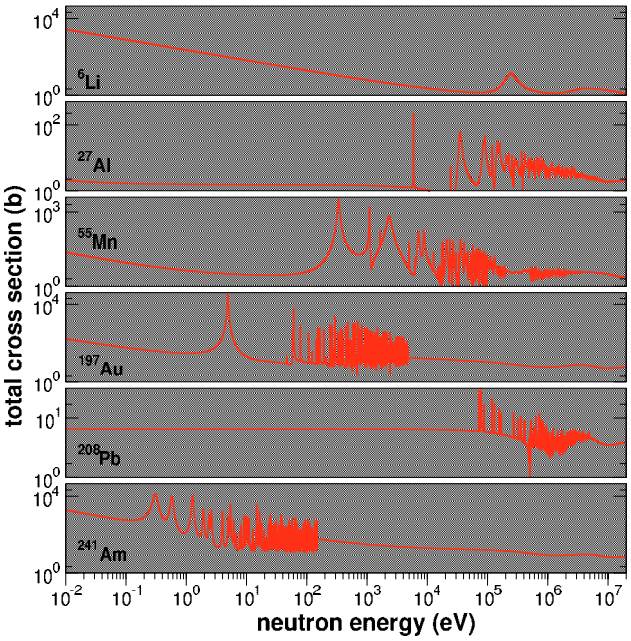

Fig. 1. Several examples of the resonance structure in the total neutron-induced reaction cross section. The general trend of increasing level density with increasing excitation energy can be observed on the the logarithmic energy scale. At the closed shell nucleus ^{208}Pb the lower level density is clearly visible.

are stored as a set of physical properties for each nuclear level excited by the incident neutron, which are energy, spin, parity and partial widths. These data allow the reconstruction of the resonance cross sections, capture, scattering, total and if applicable fission, at any given target temperature. The URR data are stored as point-wise cross sections for all possible reactions in the form of interpolation tables.

Considerable efforts have been made to produce coherent and consistent evaluated nuclear data files of high quality, reflecting as much as possible the inherent physical properties in order to be truly multi-purpose. Improved nuclear model calculations as well as new experimental data from existing and new experimental facilities have contributed largely to this result. The improvement of the quality of these neutron cross section libraries rely among others on the availability of accurate measurements obtainable at advanced neutron sources.

In the next section we will give an overview of the experimental activities at the neutron time-of-flight facility n_TOF at CERN in Geneva, commissioned in 2001 for the study of neutron induced reactions for nuclear technology, nuclear astrophysics, and nuclear structure and reaction physics. Up to now, the facility has been mainly used to measure neutron capture and fission cross sections of a large number of isotopes.

2 The neutron time-of-flight facility n_TOF at CERN

The construction and commissioning of a new neutron time-of-flight facility at CERN, after an idea proposed by Rubbia

et al. [25], was finished in 2001. The facility has become fully operational with the start of the scientific measurement programme in May 2002.

The facility delivers neutrons produced by spallation reactions induced by a pulsed, 6 ns wide, 20 GeV/c proton beam with up to 7×10^{12} protons per pulse, impinging on a $80 \times 80 \times 60\,\mathrm{cm}^3$ lead target, yielding about 300 neutrons per incident proton. A 5 cm water slab surrounding the lead target serves as a coolant and at the same time as a moderator of the initially fast neutron spectrum, providing a wide energy spectrum from thermal to about 250 MeV with a nearly $1/E$ isolethargic flux dependence from 1 eV up to 1 MeV. A vacuum neutron beam line leads to the experimental area at 185 m from the lead target. A full description of the characteristics and performances of the facility is described elsewhere [26]. An outline will be given here.

The neutron beam is obtained by means of two collimators, consisting of layers of iron and borated polyethylene. The iron serves to stop fast neutrons, while the hydrogen in polyethylene moderates the neutrons, and ^{10}B captures the slower neutrons. The first collimator has an inner diameter of 11 cm, an outer diameter of 50 cm and is placed at 135 m from the lead target. The second collimator is located near the experimental area at a distance of 175 m and has an outer diameter of 40 cm a variable inner diameter. Typically an inner diameter of 1.8 cm is used for capture measurements and 8 cm for fission experiments. This collimation results in a nearly symmetric Gaussian-shaped beam profile at the sample position with a standard deviation of about 0.77 cm at low neutron energies with the 1.8 cm diameter collimator. The spatial distribution has been accurately measured and modelled as a function of neutron energy [27].

In order to remove residual charged particles going along the neutron beam line, a 1.5 T sweeping magnet has been placed at a distance of 145 m of the spallation target. A previously observed background, presumably due to capture of negative muons, has been drastically reduced by means of a 3 m thick iron shielding located just after the sweeping magnet [28,29]. The experimental area where the samples and detectors are mounted for capture and fission experiments ranges from 182 to 190 m. It will be described in more detail in the next section. The neutron beam line is extended for an additional 12 m beyond the experimental area to minimize the background from back-scattered neutrons.

In order to perform background measurements by filtering the neutron beam at specific energies by means of the black resonance method, a multifilter changer has been installed in the beam line upstream of the first collimator.

The neutron kinetic energy is determined by time of flight. This is possible since the proton beam is pulsed. The impact of the proton beam on the lead target is closely related to the creation time of neutrons of all energies. The detection of a reaction product of a neutron-induced reaction in the experimental area provides the time the neutron has taken to travel the distance from the spallation target to the experimental area. The velocity and hence the kinetic energy of the neutron can be deduced from the flight time and the flight distance. The repetition period of the proton pulses is at least 2.4 seconds, which is low enough to cover the energy range down to subthermal energies and to prevent overlapping of slow neutrons in subsequent cycles.

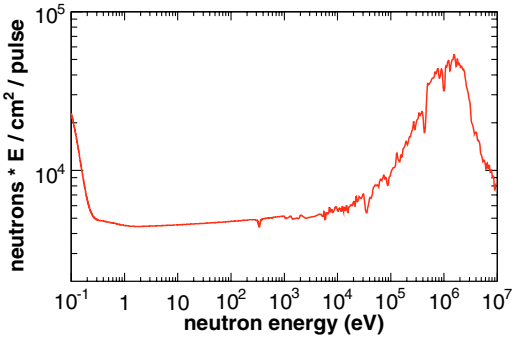

Fig. 2. The neutron flux respresented as the number of neutrons per cm^2 at the sample position of 185 m per standard pulse of 7×10^{12} protons.

2.1 Beam characteristics

A pulsed white neutron source is characterized by the energy distribution of its neutron flux, both time-averaged and per time-of-flight bunch, but also by its energy resolution. The energy distribution of the neutron flux at the sample position at 185 m for a standard time-of-flight bunch of 7×10^{12} protons is shown in figure 2. The data are based on a measurement performed with a ^{235}U loaded parallel plate fission ionization chamber from the Physikalisch-Technische Bundesanstalt in Braunschweig [30], and below 1 keV from a ^{6}Li-based in-beam neutron flux monitor [31]. The ^{6}Li-based flux detector is always present during the measurements. The flux per bunch governs the signal to noise ratio. In capture experiments a high flux per bunch results in a favorable ratio of gamma rays from (n,γ) reactions to gamma rays from radioactivity. In order to obtain the average flux, which is relevant for the duration of the experiment, one just multiplies the instantaneous flux with the repetition rate of the proton beam.

At higher neutron energies the reaction cross sections do not show the resonance structure anymore and have a smooth behaviour. Therefore an approximate knowledge of the energy resolution is sufficient. At lower energies in the resolved resonance region however the cross section can vary several orders of magnitude over a few electronvolt. There the full distribution of the energy resolution, which is often non-Gaussian, is needed to determine accurately the description of the resonances.

The resolution in energy for a measured flight time can conveniently be expressed in terms of a spread in the effective flight distance. The distribution of this equivalent distance is an appropriate quantity to evaluate the resolution as a function of neutron energy. We obtained the resolution function of the n_TOF facility by two independent simulation codes giving consistent results [32,33]. The Monte Carlo results were then fitted by an analytical two-dimensional function and implemented in the resonance shape analysis code SAMMY [34]. In figure 3 the resolution function in the form of the equivalent distance distribution is shown in the relevant energy range from 1 eV to 1 MeV on a logarithmic scale.

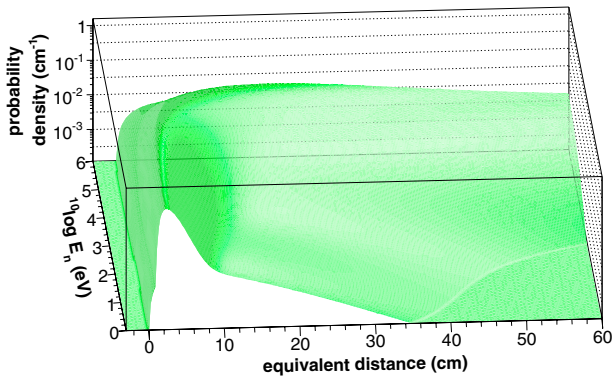

Fig. 3. The resolution function of the n_TOF facility represented as the distribution of the equivalent distance as a function of the neutron energy.

2.2 Detectors and data acquisition

Several detectors have been used during the first phase of data taking from 2002 to 2004 for the capture and fission experiments.

In-house developed deuterated benzene C_6D_6 gamma-ray detectors contained in a cylindrical low mass carbon fibre housing [35] have been used for neutron capture measurements on several isotopes. The samples were kept in position by a carbon fiber sample changer. The low neutron capture cross sections of both carbon and deuterium assure a low contribution from sample scattered neutrons to the background. Since this detector does not measure the full gamma-ray cascade following neutron capture, it requires the use of weighting functions to reconstruct the neutron capture yield [36,37]. Although the detection efficiency for a single detector is only about 3% for a 1 MeV gamma-ray, due to the gamma-ray multiplicity after neutron capture, the efficiency to detect a capture event is roughly 20% for the set of two detectors.

A second neutron capture detector has become availabe in 2004 [38–40]. It consists of a 4π 100% efficiency total absorption capture detector, made up of 40 BaF_2 crystals contained in ^{10}B loaded carbon fibre capsules, coupled to XP4512B photomultipliers equipped with for this purpose designed voltage dividers. Samples are surrounded by a $C_{12}H_{20}O_4(^6Li)_2$ neutron absorber which moderates and absorbs sample scattered neutrons. The ensemble is placed in the center of the calorimeter. Since this detector is used to select the total gamma-ray cascade from neutron capture, it can distinguish gamma rays originating from other processes.

For the capture measurements the reaction yields are normalized either to the cross section of ^{197}Au(n,γ), which is a standard in the energy region above 200 keV, or to a low-energy saturated resonance in a ^{197}Au reference sample or in the sample to be measured itself.

Fission experiments have been performed with two different detector systems. Two Fission Ionization Chambers (FIC) have been developed for use at the n_TOF facility using deposits of fissile isotopes on 100 μm thick aluminum foils. The FIC-0 detector was used for the low activity samples while the FIC-1 detector was used for the samples with higher activity [41].

The second type of fission detector is based on Parallel Plate Avalanche Counters (PPACs), developed with target deposits on 1.5 μm thin mylar or 2 μm aluminum foils, allowing to detect the two fission fragments in coincidence [42].

In both fission detectors the cross sections are determined relative to the ^{235}U(n,f) standard, measured in the same detector.

The relative incident neutron flux, i.e. the shape of the neutron kinetic energy distribution of the flux, is continuously measured during the experiments with the previously described ^{6}Li-based flux detector [31]. In addition, three $^{10}BF_3$ detectors are installed in the neutron escape line for monitoring purposes.

The data acquisition system [43] is based on the sampling of the detector signals in order to extract the deposited energy and the time of flight. An array of 54 Acqiris flash ADCs with 8 bit amplitude resolution and 1 ns sampling interval with 8 Mbytes of memory was used to record the full detector signal following the start time given by the incident protons.

The digitizers were operated at 500 Msamples/s allowing to store the detector signal during 16 ms, corresponding to a time-of-flight of 0.7 eV. Sampling the full detector signal after the neutron burst allows to fully eliminate the dead time related to the signal recording. An effective value of the dead time of about 25 nanoseconds, for which a correction is applied, is related to the software for pulse extraction. After zero suppression, the data are transferred to CERNs data storage facility CASTOR for off-line analysis with dedicated pulse shape analysis routines for each detector.

3 Cross secion measurements

During the first phase of data taking two types of cross section experiments have been performed, neutron capture cross section measurements with the C_6D_6 and BaF_2 detectors, and neutron induced fission measurements with the FIC and PPAC detectors. A summary of these measurements is given in table 1.

Capture measurements with the C_6D_6 detectors concerned ^{24,25,26}Mg, ^{56}Fe, ^{90,91,92,93,94,96}Zr [44], ^{139}La [45], ^{151}Sm [46, 47], ^{186,187,188}Os [48], ^{197}Au [49], ^{204}Pb [50], ^{206}Pb [51], ^{207}Pb [52], ^{208}Pb, ^{209}Bi [53,54], and ^{232}Th [55]. The BaF_2 4π calorimeter has been used for measurements of ^{197}Au [49], ^{233}U [39], ^{234}U [40], and ^{237}Np, ^{240}Pu, and ^{243}Am [38].

Several of these measurements are still under analysis, while for others final data have been published. The only fissile isotope that has been measured during this campaign is

Table 1. Summary of the measurements performed during the first phase of data taking at n_TOF at CERN.

detector	measured isotopes
C_6D_6 (capture)	^{24,25,26}Mg, ^{56}Fe, ^{90,91,92,93,94,96}Zr, ^{139}La,^{151}Sm, ^{186,187,188}Os, ^{197}Au, ^{204,206,207,208}Pb, ^{209}Bi, ^{232}Th
BaF_2 (capture)	^{197}Au, ^{233,234}U, ^{237}Np, ^{240}Pu, ^{243}Am
FIC (fission)	^{232}Th, ^{237}Np, ^{233,234,235,236,238}U, ^{241,243}Am, ^{245}Cm
PPAC (fission)	^{nat}Pb, ^{209}Bi, ^{232}Th, ^{237}Np,^{233,234,235,238}U

^{233}U, as a test to distinguish between gamma rays originating from capture and fission reactions. Most of the radioactive samples could not be used in mass-less supports because of safety regulations but had to be contained in titanium cannings.

Capture experiments are generally performed with one sample in the beam per measurement. The sample masses can be relatively high without disturbing the measurement. For fission experiments on the contrary, the samples should be thin enough so that fission fragments can leave the sample and be detected. For this reason the available mass is therefore best divided over a larger surface. These thin samples allow the measurement of several different isotopes simultaneously.

The fission cross sections measured with the FIC-0 detector were the isotopes ^{232}Th, ^{234}U, ^{235}U, ^{236}U, ^{238}U, and ^{237}Np, while the isotopes ^{233}U, ^{235}U, ^{238}U ^{241}Am, ^{243}Am, and ^{245}Cm were measured in the ISO-2919 compliant FIC-1 detector. An overview and status of the analysis given in ref. [41].

With the fission detectors based on Parallel Plate Avalanche Counters (PPACs) cross sections of ^{nat}Pb, ^{209}Bi, ^{232}Th, ^{237}Np, ^{233}U, ^{234}U, ^{235}U, ^{238}U have been measured, as described in more detail in ref. [42].

4 Concluding remarks

After the successful completion of data taking during the first phase of the n_TOF facility from 2002 to 2004, the installation has not been running in the period 2005–2007. An upgrade of the infrastructure of the facility is expected in 2007 and a new series of capture and fission measurements is planned for a second phase of operation. On the longer term, we plan to construct a second flight path at the shorter distance of 20 m for a third phase. In view of this purpose, several studies for a possible new spallation target have been performed, see for example ref. [56].

Capture measurements on radioactive isotopes take advantage of the high instantaneous flux at the n_TOF facility while both capture and fission measurements benefit from the large energy range that can be measured in a single experiment. One of the challenges to be addressed in the near future is the improvement of the measurement of capture in presence of fission. Capture measurements of fissile isotopes will need considerable detector developments.

The short flight path with an increased flux of about a factor of hundred allows to perform measurements with very low mass samples and opens a wide range of new possibilities for neutron time-of-flight measurements.

This work has been supported by the European Commission's 5th Framework Programme under contract No. FIKW-CT-2000-00107 (n_TOF-ND-ADS).

References

1. G. Wallerstein et al., Rev. Mod. Phys. **69**, 995 (1997).
2. F. Käppeler, Progr. Particle Nucl. Phys. **43**, 419 (1999).
3. G.E. Mitchell, J.D. Bowman, H.A. Weidenmüller, Rev. Mod. Phys. **71**, 445 (1999).
4. Y. Masuda et al., Nucl. Phys. A **721**, 485C (2003).
5. T.v. Egidy, D. Bucurescu, Phys. Rev. C **72**, 044311 (2005).
6. H. Nakamura, T. Fukahori, Phys. Rev. C **72**, 064329 (2005).
7. W.P. Abfalterer, R.W. Finlay, S.M. Grimes, Phys. Rev. C **62**, 064312 (2000).
8. M. Salvatores, I. Slessarev, A. Tchistiakov, Nucl. Sci. Eng. **130**, 309 (1998).
9. W. Gudowski, Nucl. Phys. A **654**, 436c (1999).
10. S. David, A. Billebaud, M.E. Brandan, R. Brissot, A. Giorni, D. Heuer, J.M. Loiseaux, O. Meplan, H. Nifenecker, J.B. Viano et al., Nucl. Instrum. Meth. Phys. Res. A **443**(2–3), 510 (2000).
11. A. Bidaud, Ph.D. thesis, University Paris XI, Orsay (2005).
12. J.E. Lynn, *The Theory of Neutron Resonance Reactions* (Clarendon Press, Oxford, 1968).
13. R.U. Haq, A. Pandey, O. Bohigas, Phys. Rev. Lett. **48**(6), 1086 (1982).
14. O. Bohigas, M.J. Giannoni, C. Schmit, Phys. Rev. Lett. **52**, 1 (1984).
15. M.L. Mehta, *Random matrices* (Academic Press, 1991).
16. A.M. Lane, R.G. Thomas, Rev. Mod. Phys. **30**, 257 (1958).
17. A.A. Luk'yanov, N.B. Yaneva, Phys. Part. Nucl. **28**, 331 (1997).
18. F. Fröhner, Tech. Rep. JEFF Report 18, OECD/NEA (2000).
19. C.R. Brune, Phys. Rev. C **66** (044611) (2002).
20. F. Gunsing, A. Leprêtre, C. Mounier, C. Raepsaet, A. Brusegan, E. Macavero, Phys. Rev. C **61** (054608), 1 (2000).
21. U. Agvaanluvsan, G.E. Mitchell, J.F.S. Jr., M.P. Pato, Nucl. Instrum. Meth. A **498**, 459 (2004).
22. S.I. Sukhoruchkin, Z.N. Soroko, V.V. Deriglazov, *Low Energy Neutron Physics, Volume I/16B, 16C, Tables of Neutron Resonance Parameters* (Springer, Landolt-Börnstein, 1998, 2004).
23. S.F. Mughabghab, *Atlas of Neutron Resonances* (Elsevier, 2005).
24. See for example the International Atomic Energy Agency (IAEA) on www-nds.iaea.org, or the OECD Nuclear Energy Agency on www.nea.fr.
25. C. Rubbia et al., Tech. Rep. CERN/LHC/98-02, CERN (1998).
26. U. Abbondanno et al., Tech. Rep. CERN-SL-2002-053 ECT (2003).
27. J. Pancin et al., Nucl. Instrum. Meth. Phys. Res. Sect. A **524**, 102 (2004).
28. U. Abbondanno et al., Tech. Rep. CERN/INTC 2001-038 (2001).
29. A. Ferrari, C. Rubbia, V. Vlachoudis, Tech. Rep. CERN-SL-EET-2001-036, CERN (2002).
30. C. Borcea et al., Nucl. Instrum. Meth. Phys. Res. Sect. A **513**, 524 (2003).
31. S. Marrone et al., Nucl. Instrum. Meth. Phys. Res. Sect. A **517**, 389 (2004).
32. C. Coceva, M. Frisoni, M. Magnani, A. Mengoni, Nucl. Instrum. Methods Phys. Res. Sect. A **489**, 346 (2002).
33. V. Vlachoudis (2002) (private communication).
34. N.M. Larson, SAMMY, Computer code Report ORNL/TM-9179/R7, Oak Ridge National Laboratory (2006).
35. R. Plag et al., Nucl. Instrum. Meth. Phys. Res. Sect. A **496**, 425 (2003).
36. J.L. Tain, F. Gunsing, D. Cano-Ott, N. Colonna, C. Domingo, E. González, M. Heil, F. Käppeler, S. Marrone, P. Mastinu et al., J. Nucl. Sci. Techn. Supp 2, p. 689 (2002).
37. A. Borella, G. Aerts, F. Gunsing, M. Moxon, P. Schillebeeckx, R. Wynants, Nucl. Instrum. Meth. Phys. Res. Sect. A: Accelerators, Spectrometers, Detectors and Associated Equipment **577**(3), 626 (2007).

38. C. Guerrero et al. (n_TOF Collaboration), *The neutron capture cross sections of $^{237}Np(n,\gamma)$ and $^{240}Pu(n,\gamma)$ and its relevance in the transmutation of nuclear waste* (these proceedings).
39. C. Lampoudis et al. (n_TOF Collaboration), *The ^{234}U neutron capture cross section measurement at the n_TOF facility* (these proceedings).
40. E. Berthoumieux et al. (n_TOF Collaboration), *Simultaneous measurement of the neutron capture and fission yields of ^{233}U* (these proceedings).
41. M. Calviani et al. (n_TOF Collaboration), *Measurement of the neutron induced fission of ^{235}U, ^{233}U and ^{245}Cm with the FIC detector at CERN n_TOF facility* (these proceedings).
42. L. Audouin et al. (n_TOF Collaboration), *Neutron-induced fission cross sections measurements at n_TOF* (these proceedings).
43. U. Abbondanno et al., Nucl. Instrum. Meth. Phys. Res. Sect. A **538**, 692 (2005).
44. G. Tagliente et al. (n_TOF Collaboration), *Measurement of the $^{90,91,92,93,94,96}Zr(n,\gamma)$, $^{139}La(n,\gamma)$ cross-sections at n_TOF* (these proceedings).
45. R. Terlizzi, U. Abbondanno, G. Aerts, H. Alvarez, F. Alvarez-Velarde, S. Andriamonje, J. Andrzejewski, P. Assimakopoulos, L. Audouin, G. Badurek et al. (n_TOF Collaboration), Phys. Rev. C (Nucl. Phys.) **75**(3), 035807 (15) (2007).
46. U. Abbondanno, G. Aerts, F. Alvarez-Velarde, H. Alvarez-Pol, S. Andriamonje, J. Andrzejewski, G. Badurek, P. Baumann, F. Becvar, J. Benlliure et al. (n_TOF Collaboration), Phys. Rev. Lett. **93**(16), 161103 (5) (2004).
47. S. Marrone, U. Abbondanno, G. Aerts, F. Alvarez-Velarde, H. Alvarez-Pol, S. Andriamonje, J. Andrzejewski, G. Badurek, P. Baumann, F. Becvar et al. (n_TOF Collaboration), Phys. Rev. C (Nucl. Phys.) **73**(3), 034604 (18) (2006).
48. K. Fujii et al. (n_TOF Collaboration), *Capture cross section measurements of $^{186,187,188}Os$ at n_TOF, the resolved resonance region* (these proceedings).
49. C. Massimi et al. (n_TOF Collaboration), *Measurement of the $^{197}Au(n,\gamma)$ cross section at n_TOF: towards a new standard* (these proceedings).
50. C. Domingo-Pardo, U. Abbondanno, G. Aerts, H. Alvarez-Pol, F. Alvarez-Velarde, S. Andriamonje, J. Andrzejewski, P. Assimakopoulos, L. Audouin, G. Badurek et al. (n_TOF Collaboration), Phys. Rev. C (Nucl. Phys.) **75**(1), 015806 (9) (2007).
51. C. Domingo-Pardo et al. (n_TOF Collaboration) (submitted to Phys. Rev. C) (2007).
52. C. Domingo-Pardo, U. Abbondanno, G. Aerts, H. Alvarez-Pol, F. Alvarez-Velarde, S. Andriamonje, J. Andrzejewski, P. Assimakopoulos, L. Audouin, G. Badurek et al. (n_TOF Collaboration), Phys. Rev. C (Nucl. Phys.) **74**, 055802 (6) (2006).
53. C. Domingo-Pardo, U. Abbondanno, G. Aerts, H. Alvarez-Pol, F. Alvarez-Velarde, S. Andriamonje, J. Andrzejewski, P. Assimakopoulos, L. Audouin, G. Badurek et al. (n_TOF Collaboration), Phys. Rev. C (Nucl. Phys.) **74**, 025807 (10) (2006).
54. C. Domingo-Pardo et al. (n_TOF Collaboration), *Improved lead and bismuth (n,γ) cross sections and their astrophysical impact* (these proceedings).
55. G. Aerts, U. Abbondanno, H. Alvarez, F. Alvarez-Velarde, S. Andriamonje, J. Andrzejewski, P. Assimakopoulos, L. Audouin, G. Badurek, P. Baumann et al. (n_TOF Collaboration), Phys. Rev. C (Nucl. Phys.) **73**, 054610 (10) (2006).
56. C. Carrapiço et al. (n_TOF Collaboration), *Design study for a new spallation target of the n_TOF facility at CERN* (these proceedings).